

Technical Note

## Usefulness of automated tractography for outcome prediction in patients with recurrent stroke

TETSUO KOYAMA, MD, PhD<sup>1, 2)\*</sup>, MIDORI MOCHIZUKI, MD<sup>1, 3)</sup>, YUKI UCHIYAMA, MD, PhD<sup>2)</sup>, KAZUHISA DOMEN, MD, PhD<sup>2)</sup>

<sup>1)</sup> Department of Rehabilitation Medicine, Nishinomiya Kyoritsu Neurosurgical Hospital: 11-1 Imazu-Yamanaka-cho, Nishinomiya-shi, Hyogo 663-8211, Japan

<sup>2)</sup> Department of Rehabilitation Medicine, School of Medicine, Hyogo Medical University, Japan

<sup>3)</sup> Present address: Department of Rehabilitation Medicine, Showa University Hospital, Japan

**Abstract.** [Purpose] To examine the usefulness of automated tractography for predicting outcomes in patients with recurrent stroke. [Participants and Methods] Diffusion tensor imaging was performed in the second week after stroke, and fractional anisotropy was calculated using automated tractography. Three patients with recurrent strokes were included in this study. [Results] Initial computed tomography findings of a 62-year-old man with stuttering speech revealed a hemorrhage in the left thalamus. Fractional anisotropy indicated slight neural damage in the association fibers of both hemispheres. The patient returned to work with mild attention deficit and aphasia. Initial diffusion-weighted imaging of a 75-year-old man with right upper extremity paresis showed high-intensity areas in the left corona radiata. Fractional anisotropy indicated bilateral neural damage to the corticospinal tract. The patient was discharged with severe right upper extremity impairment and a modified gait. Initial diffusion-weighted imaging of a 60-year-old woman with moyamoya disease who experienced a sudden loss of consciousness showed high-intensity areas in the left anterior circulation territories. Fractional anisotropy indicated severe damage to the right hemisphere, the corticospinal tract, and the superior longitudinal fasciculus of the left hemisphere. She was transferred to a nursing home and remained bedridden. [Conclusion] The symptoms identified in this study agreed with automated tractography findings, which suggests that this methodology is useful for predicting recurrent stroke outcomes.

**Key words:** Magnetic resonance imaging, Prognosis, Recovery

(This article was submitted Jun. 18, 2024, and was accepted Jul. 23, 2024)

## INTRODUCTION

Outcome prediction is important when planning rehabilitative regimens for stroke patients<sup>1)</sup>. Among the neuroimaging techniques that have been suggested for this purpose<sup>2)</sup>, diffusion-tensor imaging (DTI) is unique in its ability to assess the integrity of the neural tracts *in vivo*<sup>3)</sup>. However, most of the relevant studies have included only patients with first-ever stroke<sup>4)</sup>, partly because assessment of pre-existing neural damage in cases of recurrent stroke is too complex to be integrated into outcome prediction models<sup>5)</sup>.

Tractography is a DTI-based procedure that illustrates the neural tracts in the brain. Traditionally, tractography has been time-consuming and labor-intensive during the preparation stages, resulting in low reproducibility. An automated procedure known as XTRACT has been developed to address this concern<sup>6)</sup>. This method uses predetermined parameter settings for tractography analyses (e.g., seed and target voxels), allowing depiction of representative neural tracts. We have previously

\*Corresponding author. Tetsuo Koyama (E-mail: koyama.t@nk-hospital.or.jp)

©2024 The Society of Physical Therapy Science. Published by IPEC Inc.



This is an open-access article distributed under the terms of the Creative Commons Attribution Non-Commercial No Derivatives (by-nc-nd) License. (CC-BY-NC-ND 4.0: <https://creativecommons.org/licenses/by-nc-nd/4.0/>)

reported on the clinical usefulness of this automated tractography technique in clinical rehabilitation settings<sup>7-11</sup>). However, in line with the existing literature, the samples in our previous studies were limited to patients with first-ever stroke.

The present study aimed to extend the clinical usefulness of the automated tractography technique to a more general population of stroke patients. We specifically focused on patients with recurrent stroke and assessed the clinical utility of automated tractography in terms of outcome prediction.

## PARTICIPANTS AND METHODS

This study is an extension of our series assessing the clinical usefulness of automated tractography in stroke patients<sup>7-11</sup>). We sampled patients with hemorrhagic or ischemic stroke who were treated at Nishinomiya Kyoritsu Neurosurgical Hospital between April 2022 and March 2024. Patients were transferred to our hospital shortly after stroke onset and underwent computed tomography and magnetic resonance imaging of the brain, including diffusion-weighted and fluid-attenuated inversion recovery (FLAIR) imaging. The image acquisition protocols used to obtain these scans were detailed in our previous reports<sup>12, 13</sup>). The study protocol was approved by the Institutional Review Board of Hyogo Medical University (approval number 4666), and informed consent was obtained via the opt-out route. To assess the clinical usefulness of automated tractography in rehabilitation after recurrent stroke, we selected three patients with recurrent stroke who had pre-existing stroke lesions in the right hemisphere and had re-presented with stroke lesions in the left hemisphere. For clarity, we focused on three patients with modified Rankin Scale (mRS) scores<sup>14</sup>) of 1, 3, and 5, indicating different final outcomes.

In line with our previous research<sup>7-11</sup>), the patients underwent DTI during the second week following admission to our acute care unit. The scans were obtained using a 3.0-Tesla Magnetom Trio scanner (Siemens AG, Erlangen, Germany) equipped with a 32-channel head coil. The DTI data were collected using a single-shot echo-planar imaging sequence directed from anterior to posterior that consisted of 30 images with non-collinear diffusion gradients ( $b=1,500$  s/mm<sup>2</sup>) and one image without diffusion weighting ( $b=0$  s/mm<sup>2</sup>). For each patient, 80 contiguous axial slices were gathered with a field of view of 256 mm × 256 mm, an acquisition matrix of 128 × 128, and a slice thickness of 2 mm. The imaging parameters included an echo time of 96 ms, a repetition time of 10,900 ms, and a flip angle of 90°. To correct for distortions caused by eddy currents and echo-planar imaging, two additional non-diffusion-weighted images were acquired in both the anterior-to-posterior and posterior-to-anterior directions. We also acquired T1-weighted images using a three-dimensional fast gradient echo sequence to capture the anatomical structure of the brain in detail. Each patient underwent acquisition of 176 contiguous sagittal slices with a field of view of 256 mm × 256 mm, an acquisition matrix of 256 × 256, and a slice thickness of 1 mm. The imaging parameters for these T1-weighted scans included an echo time of 2.52 ms, a repetition time of 1,900 ms, and a flip angle of 10°.

The imaging protocol has been described in detail elsewhere<sup>7-11</sup>). Briefly, the initial steps involved removing Gibbs ringing artifacts, correcting distortions from eddy currents and echo-planar imaging, and applying bias field corrections using MRtrix software<sup>15</sup>) and the FMRIB Software Library<sup>16</sup>). Brain masks were then generated from the bias field-corrected images. Following this preparatory phase, fiber tracking was conducted using the BEDPOSTX and the XTRACT tool<sup>6</sup>) in the FMRIB Software Library<sup>16</sup>), which allowed creation of tractography for 42 predefined neural bundle sets. Parameter estimates, including fractional anisotropy (FA) values, were obtained with a threshold set at 0.01, as in our previous studies<sup>7-11</sup>). We focused on neural tracts commonly affected by stroke<sup>11</sup>), namely, the corticospinal tract, the superior longitudinal fasciculus parts 1, 2, and 3 (SLF1-3), the frontal aslant tract, the cingulum bundle, the anterior thalamic radiation, the arcuate fasciculus, the inferior fronto-occipital fasciculus, the inferior longitudinal fasciculus, and the uncinata fasciculus.

Damage to neural tracts was evaluated by taking the distribution of FA values in the contralateral non-lesioned hemisphere for corresponding tracts as a normative reference<sup>11</sup>). This procedure included patients who had experienced their first-ever stroke, had a supratentorial and unilateral lesion in the cerebral hemisphere, and were functionally independent in activities of daily living (ADL) before the stroke. During the study period, we collected data from our analytical database on 158 stroke patients with a lesion in the left hemisphere ( $n=76$ ) or right hemisphere ( $n=82$ ). Accordingly, we obtained 76 samples from the non-lesioned right hemisphere and 82 from the non-lesioned left hemisphere. Data for the selected tracts were summarized as the mean ± standard deviation (Table 1). Using these normative values, we calculated Z-scores for the FA of each neural tract<sup>11</sup>). In this study, these Z-scores were used as an index of neural tract damage. Neural tracts with Z-scores smaller than -1.96 were regarded as potentially damaged<sup>11</sup>).

Clinical manifestations were assessed as follows. Extremity functions were evaluated using the Brunnstrom Recovery Stage (BRS) score (1, null; 6, full)<sup>17</sup>) or the Medical Research Council (MRC) score (0, null; 5, full)<sup>18</sup>). These scores include three components, namely, the proximal and distal portions of the upper extremity and the entire lower extremity. Disability in ADL was assessed using either the Functional Independence Measure (FIM)<sup>17</sup>) or mRS score<sup>14</sup>). The FIM is widely used for assessment of independence in ADL and consists of a motor component with 13 items and a cognition component with 5 items. Each item is rated on a 7-point scale, where 1 indicates complete dependence and 7 indicates complete independence. The total scores for FIM-motor (ranging from 13 to 91) and FIM-cognition (ranging from 5 to 35) are frequently used in stroke rehabilitation assessments. Meanwhile, the mRS focuses mainly on locomotive disability, with scores ranging from 0 (normal walking) to 5 (bedridden).

## RESULTS

Three patients with previous stroke lesions in the right hemisphere and current stroke lesions in the left hemisphere were investigated. [Figure 1](#) shows the brain images obtained at the time of their arrival at our acute care service. The DTI acquisition series were conducted uneventfully in all three patients, and tractography analyses were successfully performed. The estimated neural tracts are shown in [Fig. 2](#) and their FA values in [Table 2](#).

**Table 1.** Distribution of fractional anisotropy values in the non-lesioned hemisphere in stroke patients

Tract	Right hemisphere (n=76)	Left hemisphere (n=82)
CST	0.590 ± 0.036	0.584 ± 0.035
SLF1	0.433 ± 0.036	0.427 ± 0.043
SLF2	0.385 ± 0.031	0.365 ± 0.038
SLF3	0.413 ± 0.039	0.404 ± 0.042
FAT	0.412 ± 0.037	0.406 ± 0.040
CB	0.440 ± 0.044	0.462 ± 0.046
ATR	0.414 ± 0.042	0.401 ± 0.046
AF	0.468 ± 0.036	0.472 ± 0.041
IFOF	0.494 ± 0.027	0.486 ± 0.042
ILF	0.431 ± 0.034	0.423 ± 0.040
UF	0.430 ± 0.040	0.414 ± 0.045

Data are presented as the mean ± standard deviation. Data for the right hemisphere were derived from 76 patients with left hemisphere lesions and those for the left hemisphere from 82 patients with right hemisphere lesions. AF: arcuate fasciculus; ATR: anterior thalamic radiation; CB: cingulum bundle; CST: corticospinal tract; FAT: frontal aslant tract; IFOF: inferior fronto-occipital fasciculus; ILF: inferior longitudinal fasciculus; L: left; R: right; SLF1: superior longitudinal fasciculus part 1; SLF2: superior longitudinal fasciculus part 2; SLF3: superior longitudinal fasciculus part 3; UF: uncinate fasciculus.

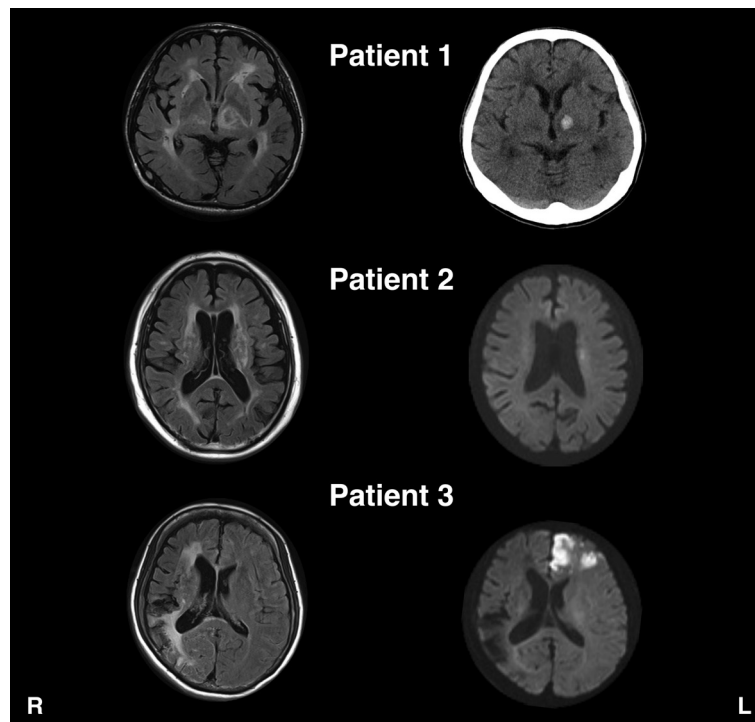


**Fig. 1.** Brain images obtained on arrival at our acute care service.

The left column shows fluid-attenuated inversion recovery images. The right column shows a computed tomography image for patient 1 and diffusion-weighted magnetic resonance images for patients 2 and 3. L: left; R: right.

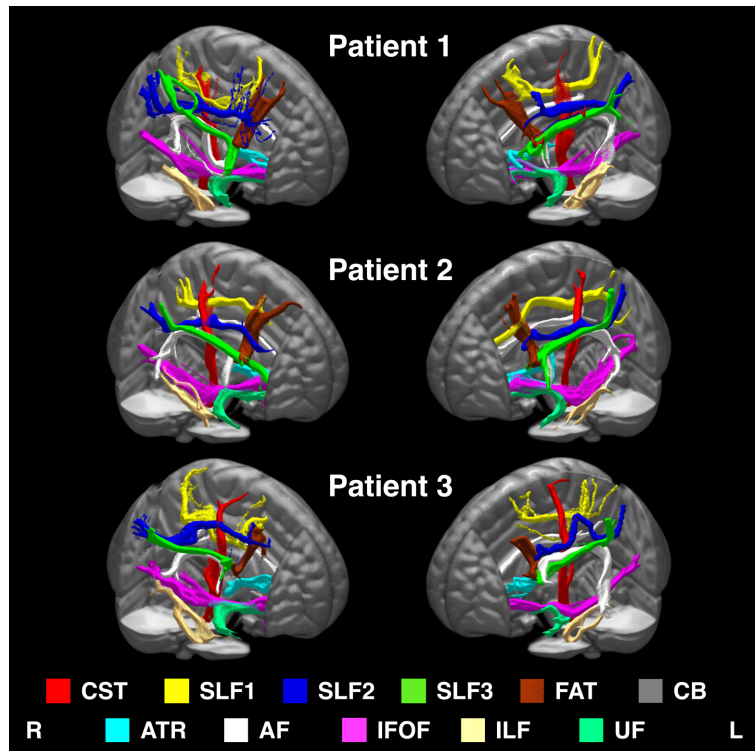


**Fig. 2.** Three-dimensional images generated by automated tractography.

AF: arcuate fasciculus; ATR: anterior thalamic radiation; CB: cingulum bundle; CST: corticospinal tract; FAT: frontal aslant tract; IFOF: inferior fronto-occipital fasciculus; ILF: inferior longitudinal fasciculus; L: left; R: right; SLF1: superior longitudinal fasciculus part 1; SLF2: superior longitudinal fasciculus part 2; SLF3: superior longitudinal fasciculus part 3; UF: uncinata fasciculus.

**Table 2.** Raw fractional anisotropy values and Z-score conversions of the neural tracts in three representative cases

Tract	Patient 1		Patient 2		Patient 3	
	Right hemisphere	Left hemisphere	Right hemisphere	Left hemisphere	Right hemisphere	Left hemisphere
CST	0.561 (Z=-0.796)	0.522 (Z=-1.783)	<b>0.459 (Z=-3.644)</b>	<b>0.448 (Z=-3.894)</b>	0.521 (Z=-1.928)	<b>0.436 (Z=-4.233)</b>
SLF1	<b>0.357 (Z=-2.117)</b>	0.406 (Z=-0.482)	0.396 (Z=-1.015)	0.398 (Z=-0.663)	<b>0.276 (Z=-4.368)</b>	<b>0.342 (Z=-1.967)</b>
SLF2	0.327 (Z=-1.868)	0.330 (Z=-0.926)	0.366 (Z=-0.655)	0.389 (Z=0.627)	<b>0.166 (Z=-6.839)</b>	<b>0.263 (Z=-2.690)</b>
SLF3	0.344 (Z=-1.778)	0.395 (Z=-0.217)	0.395 (Z=-0.468)	0.381 (Z=-0.549)	<b>0.173 (Z=-6.163)</b>	0.367 (Z=-0.880)
FAT	0.371 (Z=-1.108)	0.381 (Z=-0.620)	0.358 (Z=-1.467)	<b>0.297 (Z=-2.726)</b>	<b>0.248 (Z=-4.429)</b>	<b>0.210 (Z=-4.891)</b>
CB	0.431 (Z=-0.205)	0.453 (Z=-0.178)	0.407 (Z=-0.738)	0.437 (Z=-0.538)	0.361 (Z=-1.781)	0.443 (Z=-0.419)
ATR	0.354 (Z=-1.437)	0.316 (Z=-1.855)	<b>0.318 (Z=-2.287)</b>	0.323 (Z=-1.694)	0.344 (Z=-1.666)	0.315 (Z=-1.860)
AF	<b>0.347 (Z=-3.357)</b>	<b>0.382 (Z=-2.202)</b>	0.453 (Z=-0.421)	0.442 (Z=-0.724)	<b>0.207 (Z=-7.242)</b>	0.399 (Z=-1.759)
IFOF	<b>0.409 (Z=-3.164)</b>	<b>0.392 (Z=-2.238)</b>	0.454 (Z=-1.499)	0.477 (Z=-0.215)	<b>0.398 (Z=-3.564)</b>	0.451 (Z=-0.845)
ILF	0.365 (Z=-1.951)	0.420 (Z=-0.069)	0.423 (Z=-0.235)	0.422 (Z=-0.015)	<b>0.313 (Z=-3.460)</b>	0.430 (Z=0.184)
UF	0.420 (Z=-0.257)	0.391 (Z=-0.513)	0.455 (Z=0.619)	0.433 (Z=0.432)	<b>0.320 (Z=-2.759)</b>	0.335 (Z=-1.758)

Neural tracts with a Z-score lower than -1.96 are shown in **bold**. To evaluate neural tract damage, we initially assessed the distribution of FA values in the non-lesioned hemispheres of the 11 tracts listed in Table 1 as normative references. Next, we evaluated the FA distribution in the targeted neural tracts. To better characterize neural damage relative to normative values, we converted the FA values to Z-scores using the formula:  $Z=(X-\mu)/\sigma$ , where X represents the individual datum point,  $\mu$  is the mean of the dataset, and  $\sigma$  is the standard deviation of the dataset. Neural tracts with a Z-score below -1.96 (in the bottom 2.5% of a normal distribution) were considered potentially damaged. AF: arcuate fasciculus; ATR: anterior thalamic radiation; CB: cingulum bundle; CST: corticospinal tract; FAT: frontal aslant tract; IFOF: inferior fronto-occipital fasciculus; ILF: inferior longitudinal fasciculus; L: left; R: right; SLF1: superior longitudinal fasciculus part 1; SLF2: superior longitudinal fasciculus part 2; SLF3: superior longitudinal fasciculus part 3; UF: uncinata fasciculus.

Patient 1 was a 62-year-old man who visited our acute care service with sudden onset of stuttering speech. His past history included an ischemic stroke with slight speech difficulty that had occurred 4 years earlier. However, he had resumed being independent in ADL (mRS 1) and returned to his former work as an electrician. During the current admission, initial computed tomography in the acute care setting showed high-density areas in the left thalamus (Fig. 1). FLAIR imaging also showed multiple and widely distributed high-intensity spots in the right hemisphere. He was managed conservatively with antihypertensive medication. DTI was performed during the second week after admission, and tractography images were produced using an automated technique (Fig. 2). The raw FA values and their Z-score conversions are shown in Table 2. These values indicated potential neural damage in the right SLF1, the right arcuate and inferior fronto-occipital fasciculi, and the left arcuate and inferior fronto-occipital fasciculi. He was diagnosed with attentional deficit and aphasia (word-finding difficulty), which corresponded to the neural damage identified by automated tractography. On day 18, he was transferred to our affiliated rehabilitation hospital for continued inpatient therapy. At discharge to home on day 108, his BRS and MRC scores were full, his FIM-motor score was 91, his FIM-cognition score was 33, and his mRS score was 1. Although slight attentional deficit and mild symptoms of aphasia remained, he returned to work under the supervision of colleagues.

Patient 2 was a 75-year-old man who presented to our acute care service with sudden-onset paresis in the right upper extremity and dysarthria. Eight years earlier, he had been diagnosed with multiple lacunar infarctions in the right hemisphere, which resulted in slight hemiparesis of the left upper extremity (MRC 4). After a one-week hospitalization at our facility, during which he received conservative treatment, he regained full independence in ADL (mRS 0) and full function in the left upper extremity (MRC 5). Initial diffusion-weighted images obtained in the acute care setting revealed high-intensity areas in the left corona radiata (Fig. 1). FLAIR images showed multiple high-intensity spots in the right and left corona radiata areas. DTI was performed during the second week, and tractography images were generated using an automated technique (Fig. 2). The raw FA values and their Z-score conversions (shown in Table 2) suggested potential neural damage in the corticospinal tracts bilaterally, the right anterior thalamic radiation, and the left frontal aslant tract. Rehabilitative treatment was initiated on day 2, at which time his BRS scores were 2-2-4 on the right side and his mRS score was 4. Functioning of the left extremities remained unaffected. On day 23, he was transferred to a convalescent rehabilitation hospital in our local community. According to the medical referral letter, he was discharged to home on day 200 with BRS scores of 2-2-5 on the right side and an mRS score of 3. There were no FIM data in the referral letter.

Patient 3 was a 60-year-old woman who was transferred to our acute care service with sudden onset of loss of consciousness. Seven years earlier, she had visited a neurology clinic with numbness in her left upper and lower extremities. She had undergone radiological examinations and been diagnosed with an ischemic stroke in the right frontal lobe. She was subsequently transferred to our facility for further examinations, including angiography, and was diagnosed with moyamoya disease. She then underwent regular outpatient follow-up to monitor her condition and was prescribed antiplatelet medication. During follow-up, she had been functionally independent and continued her job as an after-school care worker. Initial diffusion-weighted imaging in the acute care setting during the current admission revealed high-intensity areas in the anterior and middle cerebral artery territories in the left hemisphere (Fig. 1). FLAIR imaging showed high-intensity areas extending throughout almost all of the right cerebral hemisphere (Fig. 1). DTI was performed during the second week, and tractography images were generated using an automated technique (Fig. 2). The findings indicated severe damage to the majority of the neural tracts in the right hemisphere and to the corticospinal tract, SLF1, SLF2, and frontal aslant tract in the left hemisphere. During hospitalization at our facility, she remained unresponsive despite her eyes being open. The BRS scores for extremity functions were 2-2-2 on both sides. A gastrostomy tube was placed for nutritional management. On day 136, she was transferred to a long-term rehabilitation facility in our local community. According to the medical referral letter, she was discharged to a nursing home on day 398 with BRS scores of 2-2-2 on both sides and an mRS score of 5. Her FIM-motor score was 13 and her FIM-cognition score was 5. Nutritional management was continued via the gastrostomy tube.

## DISCUSSION

Automated tractography has been confirmed to be a clinically useful tool for predicting the outcome of stroke<sup>7-11</sup>. Our previous studies have demonstrated that raw FA values can accurately assess symptoms and their severity<sup>7, 8</sup>. We have also demonstrated that Z-score conversion of FA serves as a clear index for assessment of neural damage<sup>11</sup>. To broaden the utility of automated tractography and encompass more challenging conditions, such as recurrent stroke, we investigated the utility of assessment of neural tracts throughout the entire brain using Z-scores<sup>11</sup>. As demonstrated in the three patients in this report, their Z-scores corresponded to the severity of their symptoms and long-term outcomes. These findings underscore the clinical usefulness of automated tractography for predicting outcomes after recurrent stroke.

It is important to note that all three patients reported here had regained functional independence in ADL following their first-ever stroke with no apparent neurological sequelae. Particularly noteworthy is that patients 1 and 3, both of whom were in their sixties, had returned to work after their initial stroke. These observations suggest that brain regions that are spared following the initial stroke may compensate for neurological dysfunction in the damaged areas<sup>19, 20</sup>. Indeed, patient 3, whose Z-scores for the neural tracts in the right hemisphere were found to be severely affected, in addition to the damage from the current stroke episode, showed minimal recovery in either extremity function or ADL. Automated tractography can be used to detect potential neural damage that does not manifest as clinical neurological symptoms after a first unilateral stroke.



In these patients, brain lesions resulting from previous strokes were identified by referencing FLAIR scans. This methodology has been widely used in previous studies of outcome prediction in stroke patients<sup>21–23</sup>. Various scaling systems, including the Fazekas scale<sup>24</sup>, have been developed for assessment of the severity of white matter lesions. However, these scaling systems typically utilize 4–7 levels of ordinal scales, which are assessed visually<sup>24, 25</sup>. This approach can result in diminished reproducibility and reduced statistical power. In contrast, FA values derived from automated tractography provide a reproducible interval scale specific to the neural tracts of interest. Use of FA values derived from automated tractography facilitates evaluation of the severity of white matter pathology before onset of the current stroke.

In real-world clinical settings, approximately 20–30 percent of stroke patients experience recurrence<sup>26–28</sup>, often resulting in more severe conditions considering the size and site of recurrent lesions, as shown in patient 3 in this report. Considering the large population of recurrent cases, outcome prediction for these patients is a crucial issue in stroke rehabilitation. In this study, based on case series methodology, we have shown that automated tractography can be useful for this issue. Future studies with a larger number of samples are needed to prove the generalizability of this technique.

This study has several limitations. First, it is important to note that FA values are contingent upon the chosen threshold. We opted for a threshold of 0.01 to be consistent with our previous tractography studies<sup>7–11</sup>. However, there is a lack of consensus within the field regarding this threshold setting. Second, although the XTRACT function automatically generates 42 neural tracts<sup>6</sup>, certain neural tracts, such as the optic radiation, were excluded from our analysis for the sake of clarity. Nevertheless, stroke patients with posterior cerebral artery involvement often present with lesions affecting these neural tracts. We intend to present data for these tracts in an upcoming case series. Third, for the sake of clarity, our study focused solely on representative cases who were functionally independent in ADL before recurrence of stroke. However, nearly half of patients have some degree of obvious neurological sequelae after a first-ever stroke<sup>29, 30</sup>. Further studies are needed in patients who required assistance in ADL before recurrence of stroke to clarify this issue.

In conclusion, the findings of this study suggest that automated tractography is useful for outcome prediction in patients with recurrent stroke.

### *Funding*

This work was partially supported by a Grant-in-Aid for Scientific Research (C) from the Japan Society for the Promotion of Science (JSPS KAKENHI Grant Number JP22K11356) and by a Grant-in-Aid for Scientific Research on Innovative Areas—Platforms for Advanced Technologies and Research Resources “Advanced Bioimaging Support” (JSPS KAKENHI Grant Number JP22H04926).

### *Conflicts of interest*

The authors declare that there are no conflicts of interest.

## REFERENCES

- 1) Stinear CM, Smith MC, Byblow WD: Prediction tools for stroke rehabilitation. *Stroke*, 2019, 50: 3314–3322. [[Medline](#)] [[CrossRef](#)]
- 2) Boyd LA, Hayward KS, Ward NS, et al.: Biomarkers of stroke recovery: consensus-based core recommendations from the stroke recovery and rehabilitation roundtable. *Neurorehabil Neural Repair*, 2017, 31: 864–876. [[Medline](#)] [[CrossRef](#)]
- 3) Puig J, Blasco G, Schlaug G, et al.: Diffusion tensor imaging as a prognostic biomarker for motor recovery and rehabilitation after stroke. *Neuroradiology*, 2017, 59: 343–351. [[Medline](#)] [[CrossRef](#)]
- 4) Kim B, Winstein C: Can neurological biomarkers of brain impairment be used to predict poststroke motor recovery? A systematic review. *Neurorehabil Neural Repair*, 2017, 31: 3–24. [[Medline](#)] [[CrossRef](#)]
- 5) Koyama T, Uchiyama Y, Domen K: Outcome in stroke patients is associated with age and fractional anisotropy in the cerebral peduncles: a multivariate regression study. *Prog Rehabil Med*, 2020, 5: 20200006. [[Medline](#)] [[CrossRef](#)]
- 6) Warrington S, Bryant KL, Khrapitchev AA, et al.: XTRACT—standardised protocols for automated tractography in the human and macaque brain. *Neuroimage*, 2020, 217: 116923. [[Medline](#)] [[CrossRef](#)]
- 7) Koyama T, Mochizuki M, Uchiyama Y, et al.: Applicability of fractional anisotropy from standardized automated tractography for outcome prediction of patients after stroke. *J Phys Ther Sci*, 2023, 35: 838–844. [[Medline](#)] [[CrossRef](#)]
- 8) Mochizuki M, Uchiyama Y, Domen K, et al.: Automated tractography for the assessment of aphasia in acute care stroke rehabilitation: a case series. *Prog Rehabil Med*, 2023, 8: 20230041. [[Medline](#)] [[CrossRef](#)]
- 9) Mochizuki M, Uchiyama Y, Domen K, et al.: Applicability of automated tractography during acute care stroke rehabilitation. *J Phys Ther Sci*, 2023, 35: 156–162. [[Medline](#)] [[CrossRef](#)]
- 10) Koyama T, Mochizuki M, Uchiyama Y, et al.: Outcome prediction by combining corticospinal tract lesion load with diffusion-tensor fractional anisotropy in patients after hemorrhagic stroke. *Prog Rehabil Med*, 2024, 9: 20240001. [[Medline](#)] [[CrossRef](#)]
- 11) Mochizuki M, Uchiyama Y, Domen K, et al.: Clinical applicability of automated tractography for stroke rehabilitation: Z-score conversion of fractional anisotropy. *J Phys Ther Sci*, 2024, 36: 319–324. [[Medline](#)] [[CrossRef](#)]
- 12) Koyama T, Marumoto K, Miyake H, et al.: Relationship between diffusion tensor fractional anisotropy and motor outcome in patients with hemiparesis after corona radiata infarct. *J Stroke Cerebrovasc Dis*, 2013, 22: 1355–1360. [[Medline](#)] [[CrossRef](#)]

- 13) Uchiyama Y, Domen K, Koyama T: Outcome prediction of patients with intracerebral hemorrhage by measurement of lesion volume in the corticospinal tract on computed tomography. *Prog Rehabil Med*, 2021, 6: 20210050. [[Medline](#)] [[CrossRef](#)]
- 14) van Swieten JC, Koudstaal PJ, Visser MC, et al.: Interobserver agreement for the assessment of handicap in stroke patients. *Stroke*, 1988, 19: 604–607. [[Medline](#)] [[CrossRef](#)]
- 15) Tournier JD, Smith R, Raffelt D, et al.: MRtrix3: A fast, flexible and open software framework for medical image processing and visualisation. *Neuroimage*, 2019, 202: 116137. [[Medline](#)] [[CrossRef](#)]
- 16) Jenkinson M, Beckmann CF, Behrens TE, et al.: FSL. *Neuroimage*, 2012, 62: 782–790. [[Medline](#)] [[CrossRef](#)]
- 17) Brunnstrom S: Motor testing procedures in hemiplegia: based on sequential recovery stages. *Phys Ther*, 1966, 46: 357–375. [[Medline](#)] [[CrossRef](#)]
- 18) Paternostro-Sluga T, Grim-Stieger M, Posch M, et al.: Reliability and validity of the Medical Research Council (MRC) scale and a modified scale for testing muscle strength in patients with radial palsy. *J Rehabil Med*, 2008, 40: 665–671. [[Medline](#)] [[CrossRef](#)]
- 19) Ward NS, Brown MM, Thompson AJ, et al.: Neural correlates of motor recovery after stroke: a longitudinal fMRI study. *Brain*, 2003, 126: 2476–2496. [[Medline](#)] [[CrossRef](#)]
- 20) Grefkes C, Ward NS: Cortical reorganization after stroke: how much and how functional? *Neuroscientist*, 2014, 20: 56–70. [[Medline](#)] [[CrossRef](#)]
- 21) Kang HJ, Stewart R, Park MS, et al.: White matter hyperintensities and functional outcomes at 2 weeks and 1 year after stroke. *Cerebrovasc Dis*, 2013, 35: 138–145. [[Medline](#)] [[CrossRef](#)]
- 22) Etherton MR, Wu O, Rost NS: Recent advances in leukoaraiosis: white matter structural integrity and functional outcomes after acute ischemic stroke. *Curr Cardiol Rep*, 2016, 18: 123. [[Medline](#)] [[CrossRef](#)]
- 23) Christidi F, Tsiptsios D, Sousanidou A, et al.: The clinical utility of leukoaraiosis as a prognostic indicator in ischemic stroke patients. *Neurol Int*, 2022, 14: 952–980. [[Medline](#)] [[CrossRef](#)]
- 24) Fazekas F, Chawluk JB, Alavi A, et al.: MR signal abnormalities at 1.5 T in Alzheimer’s dementia and normal aging. *AJR Am J Roentgenol*, 1987, 149: 351–356. [[Medline](#)] [[CrossRef](#)]
- 25) Scheltens P, Barkhof F, Leys D, et al.: A semiquantitative rating scale for the assessment of signal hyperintensities on magnetic resonance imaging. *J Neurol Sci*, 1993, 114: 7–12. [[Medline](#)] [[CrossRef](#)]
- 26) Takashima N, Arima H, Kita Y, et al. Shiga Stroke and Heart Attack Registry Group: Two-year recurrence after first-ever stroke in a general population of 1.4 million Japanese patients—the Shiga stroke and heart attack registry study. *Circ J*, 2020, 84: 943–948. [[Medline](#)] [[CrossRef](#)]
- 27) Kolmos M, Christoffersen L, Kruuse C: Recurrent ischemic stroke—a systematic review and meta-analysis. *J Stroke Cerebrovasc Dis*, 2021, 30: 105935. [[Medline](#)] [[CrossRef](#)]
- 28) Nakanishi Y, Furuta Y, Hata J, et al.: Long-term trends in the 5-year risk of recurrent stroke over a half century in a Japanese community: the Hisayama study. *J Atheroscler Thromb*, 2022, 29: 1759–1773. [[Medline](#)] [[CrossRef](#)]
- 29) Mukherjee D, Patil CG: Epidemiology and the global burden of stroke. *World Neurosurg*, 2011, 76: S85–S90. [[Medline](#)] [[CrossRef](#)]
- 30) Feigin VL, Norrving B, Mensah GA: Global burden of stroke. *Circ Res*, 2017, 120: 439–448. [[Medline](#)] [[CrossRef](#)]